HHS Public Access

Author manuscript

Cancer Cell. Author manuscript; available in PMC 2016 October 12.

Published in final edited form as:

Cancer Cell. 2015 October 12; 28(4): 429–440. doi:10.1016/j.ccell.2015.09.007.

Adult Lineage Restricted CNS Progenitors Specify Distinct Glioblastoma Subtypes

Sheila R. Alcantara Llaguno[1,4,7,*], **Zilai Wang**[1,4,7], **Daochun Sun**[1,4], **Jian Chen**[1,5], **Jing Xu**[1], **Euiseok Kim**[2,6], **Kimmo J. Hatanpaa**[3], **Jack M. Raisanen**[3], **Dennis K. Burns**[3], **Jane E. Johnson**[2], and **Luis F. Parada**[1,4,*]

[1]Department of Developmental Biology, The University of Texas Southwestern Medical Center at Dallas, Dallas, TX 75390 USA

[2]Department of Neuroscience, The University of Texas Southwestern Medical Center at Dallas, Dallas, TX 75390 USA

[3]Department of Pathology, The University of Texas Southwestern Medical Center at Dallas, Dallas, TX 75390 USA

Summary

A central question in glioblastoma multiforme (GBM) research is the identity of the tumor-initiating cell, and its contribution to the malignant phenotype and genomic state. We examine the potential of adult lineage restricted progenitors to induce fully penetrant GBM using central nervous system (CNS) progenitor-specific inducible Cre mice to mutate *Nf1, Trp53* and *Pten*. We identify two phenotypically and molecularly distinct GBM subtypes governed by identical driver mutations. We demonstrate that the two subtypes arise from functionally independent pools of adult CNS progenitors. Despite histologic identity as GBM, these tumor types are separable based on the lineage of the tumor-initiating cell. These studies point to the cell of origin as a major determinant of GBM subtype diversity.

[*]Co-corresponding authors: Luis F. Parada, luis.parada@utsouthwestern.edu / paradal@mskcc.org and Sheila R. Alcantara Llaguno, alcantas@mskcc.org.

[4]Present address: Brain Tumor Center and Cancer Biology & Genetics Program, Memorial Sloan Kettering Cancer Center, New York, NY 10065 USA

[5]Present address: Institute of Functional Nano & Soft Materials, Soochow University Jiangsu, P. R. China 215123

[6]Present address: Systems Neurobiology Laboratories, The Salk Institute for Biological Studies, La Jolla, CA 92037 USA

[7]Co-first authors

Author Contributions

S.R.A.L., Z.W., D.S., and L.F.P. designed research. S.R.A.L, Z.W., J.C. and J.X. performed experiments. S.R.A.L., Z.W., D.S., J.C., D.K.B., J.M.R., K.J.H., J.E.J., and L.F.P. analyzed data. E.K., J.E.J., J.M.R., and K.J.H. contributed new reagents/material. S.R.A.L. and L.F.P. wrote the manuscript.

The authors report no conflict of interest.

Introduction

GBM remains one of the most lethal forms of adult human cancer, with a median survival of about one year from time of diagnosis (Stupp et al., 2005; Wen and Kesari, 2008). Its invasive and rapidly progressive nature has prompted numerous studies on the origins of these highly malignant tumors. Traditionally, the concept that cancer can spontaneously develop from any or most somatic cells was widely accepted and GBM was thought to be derived from astrocytes (Sanai et al., 2005). Given the need for accumulation of multiple mutations, the unlimited self-renewal potential of stem cells would more easily allow such events during the lifetime of an individual, making them more accessible targets for malignant transformation (Chen et al., 2012b; Reya et al., 2001). Accordingly, adult stem cells have been shown to exhibit tumor-initiating potential in animal models of leukemia, breast, lung, colon and other organ cancers (Alcantara Llaguno et al., 2009; Sell, 2010; Visvader, 2011). In the brain, direct or indirect targeting of the tumor suppressors *Nf1*, *Trp53*, and *Pten* in adult mouse neural stem cells has been demonstrated to induce high-grade gliomas that faithfully phenocopy the human malignancy (Alcantara Llaguno et al., 2009; Chen et al., 2012a; Jacques et al., 2010). In the experimental setting, the transformation of more mature neural cells to form tumors has been reported, although how such a manipulation could relate to the physiological setting of gradually accumulating mutations is less clear (Friedmann-Morvinski et al., 2012).

The role of adult lineage restricted progenitors in solid tumor etiology is not well characterized. Unlike multipotent stem cells, most progenitors have limited self-renewal and are fated to differentiate into post-mitotic cells that present impediments to transformation (Huntly et al., 2004; Lillien, 1998). In hematologic malignancies, it has been shown that leukemias can arise from stem cells, myeloid, and lymphoid progenitors (Krivtsov et al., 2006). Some oncogenes, such as MOZ-TIF2 and MLL-AF9, but not BCR-ABL, transform committed hematopoietic progenitors and confer properties of stem cells, like enhanced self-renewal (Huntly et al., 2004). Other studies indicate that initiating mutations in stem cells can create leukemia of committed progenitor phenotype, indicating that progenitors can be important cellular incubators of leukemia (Cozzio et al., 2003). How these scenarios play out in the case of gliomas is not known.

In mature rodent brain, new neurons are continually produced in the adult subventricular zone (SVZ) of the lateral ventricles and the subgranular zone (SGZ) of the dentate gyrus (Alvarez-Buylla and Lim, 2004; Zhao et al., 2008). In the SVZ and SGZ, neural stem cells (NSCs) are relatively quiescent, glial fibrillary acidic protein (Gfap)-expressing cells that exhibit lifelong self-renewal potential and generate neural progenitor cells (NPCs) whose fate and terminal differentiation are rapidly achieved. NPCs are transit amplifying cells that typically undergo several rounds of cell division before forming new neurons that either migrate from the SVZ through the rostral migratory stream (RMS) and into the olfactory bulb (OB), or locally within the dentate gyrus (Doetsch et al., 1999; Zhao et al., 2008). Oligodendrocyte Progenitor Cells (OPCs), on the other hand, are broadly arrayed in the adult brain, where they constitute the largest pool of dividing cells. These cells are responsible for generating myelin-forming oligodendrocytes in the developing and mature

CNS, and are the source of myelin-forming cells following demyelinating lesions (Nishiyama et al., 2009).

In order to specifically target discrete adult progenitor populations in the brain, we used Cre transgenic mice that drive recombination in different adult CNS cell types. Specific regulatory elements of the rat Nestin gene have been harnessed to specify transgene expression to adult neural stem cells of the SVZ and SGZ (Alcantara Llaguno et al., 2009; Chen et al., 2009; Chen et al., 2012a); regulatory elements of the mouse Ascl1 gene direct recombination specifically in the SVZ and SGZ adult committed neural progenitor lineage and adult OPCs (Kim et al., 2008; Kim et al., 2007); and those of the mouse NG2 gene are specific for OPCs in the adult mouse brain (Zhu et al., 2011). In this study, we investigate the role of adult neural and oligodendrocyte progenitor cells in the development of GBM.

Results

We previously identified adult SVZ neural stem cells as an efficient source of gliomas in mouse models caused by inactivation of *Nf1*, *Trp53*, and *Pten*, three of the most commonly mutated genes in human GBM (Alcantara Llaguno et al., 2009; TCGA, 2008). In order to specifically target adult lineage restricted CNS progenitors to the exclusion of stem cells, we turned to a transgenic mouse line that expresses tamoxifen-inducible cre under the control of *Ascl1* regulatory elements (Kim et al., 2008; Kim et al., 2007; Mich et al., 2014). Using the *Ascl1-creER^{TM};R26-stop-lacZ* reporter, X-gal staining of tamoxifen-treated mouse brains verified specific recombination in the SVZ-RMS-OB and the SGZ at two weeks post-induction (Figure S1A). LacZ^{+} cells were also found in white matter and subcortical gray matter regions, including corpus callosum, hypothalamus and thalamic regions, where OPCs and their progeny are located. Immunostaining of *Ascl1-creER^{TM};R26-stop-YFP* reporter brains showed colocalization of the YFP signal with markers for adult neural and oligodendrocyte lineages (Figures 1A, S1B). YFP co-localized with neural stem and progenitor markers Sox2 and Nestin but not the stem cell-specific marker Gfap in the SVZ and SGZ (Alvarez-Buylla and Lim, 2004; Zhao et al., 2008). YFP also co-stained with the immature neuronal marker doublecortin (Dcx) and the mature neuronal marker NeuN in the RMS-OB and the dentate gyrus, as well as the OPC marker Olig2 and mature oligodendrocyte marker APC in OPC regions such as the thalamus. These data confirm the expression of the *Ascl1-creER^{TM}* transgene in a subset of adult CNS progenitors and their derivatives, but not in stem cells.

Adult Lineage Restricted CNS Progenitors Produce Glioma

To determine whether tumor suppressor deletion in adult committed progenitors also efficiently generates malignant gliomas, we bred *Ascl1-creER^{TM}* mice to incorporate conditional and/or null alleles of *Nf1*, *Trp53* and *Pten* to yield the following genotypes: *Ascl1-creER^{TM};Nf1$^{flox/flox}$;Trp53$^{flox/flox}$* or *Ascl1-creER^{TM};Nf1$^{flox/flox}$;Trp53$^{flox/-}$* (AscNP), and *Ascl1-creER^{TM};Nf1$^{flox/flox}$;Trp53$^{flox/flox}$;Pten$^{flox/+}$* (AscNPP). Adult mutants and controls were induced with tamoxifen or vehicle at 4 weeks of age. AscNP and AscNPP mice showed accelerated morbidity (Figure 1B). Furthermore, one or two tamoxifen doses

had similar tumor kinetics and median survival in AscNP mice, suggesting saturation of recombination efficiency (Figure 1C).

Analysis of symptomatic AscNP and AscNPP mice demonstrated malignant gliomas (Figure 1D–E). Hematoxylin and eosin (H&E) staining showed the classical features of diffusely infiltrating high-grade gliomas (Figure 1D), with indistinct tumor borders (Figure 1De), pseudopalisading necrosis (Figure 1Dg), and prominent mitoses (Figure 1Dh). Control mice (Figures 1Db, Dd, Df) did not develop tumors. AscNP and AscNPP tumors were classified as Grade III (anaplastic astrocytoma) or Grade IV (glioblastoma multiforme) based on the World Health Organization (WHO) classification system (Louis et al., 2007; Figure 1E). The gliomas were immunoreactive for the classical markers Ki67, Gfap, Nestin, and Olig2, as well as progenitor markers Sox2 and platelet-derived growth factor receptor α (Pdgfrα; Figure 1F). Cre-mediated tumor suppressor deletion in AscNP mice was verified by genotyping (Figure S1C), and Western analysis, showing absence of the Nf1 protein and accumulation of mutant p53 protein (Figure 1G). These data demonstrate that *Nf1*, *Trp53* and *Pten* tumor suppressor inactivation in adult lineage restricted progenitor cells is sufficient to induce malignant glioma.

In vivo, AscNP tumor cells undergo multi-lineage differentiation (Figure 1H). β-galactosidase-positive tumor cells were immunoreactive for markers of astrocytes (Gfap; S100β–data not shown), neurons (NeuN), and oligodendrocytes (myelin basic protein, Mbp). Freshly dissociated AscNP tumors grown in growth factor-supplemented, serum-free media produced tumorspheres, self-renew and undergo multi-lineage differentiation when shifted to serum-containing media (Figures S1D–E). Thus, adult progenitor-driven gliomas exhibit stem cell-like properties including self-renewal and multipotency when tested in vitro.

Early Proliferation and Migration Defects in Mutant Adult CNS Progenitors

To gain insight into the early events in glioma formation, we analyzed pre-symptomatic AscNP mice. At one month post-tamoxifen induction, no abnormal histology was detected (data not shown), but at 4 months post-induction, we observed evidence of abnormal proliferation, differentiation and migration (Figure 2). X-gal staining of AscNP mutants showed enhanced staining of recombined $lacZ^+$ cells in the adult neural and oligodendrocyte progenitor regions compared to age-matched controls (Figure 2A). In the SVZ, AscNP mice showed enhanced Ki67 and Nestin staining, as well as increased short term BrdU (5-bromo-2′-deoxyuridine) incorporation (Figures 2B–2C) and proliferation index (Figure 2D). In contrast, the AscNP SVZ appeared depleted of doublecortin (Dcx), with reduced Dcx^+ newborn neurons, but with increased number of Dcx^+ cells in their final destination, the olfactory bulb (Figures 2B, 2E). We observed no difference in apoptosis (Figure S2). These data reveal early migratory and differentiation abnormalities in AscNP adult neural progenitors.

AscNP OPCs also showed increased lacZ staining (Figure 2A) and proliferation in short-term BrdU pulse-chases (Figures 2C, 2F), as well as increased abundance of the OPC marker Olig2 (Figures 2B–2C, 2G). Thus, both mutant adult neural and oligodendrocytic progenitors exhibit enhanced proliferation, differentiation, and migration alterations in advance of obvious tumor formation.

AscNP and NPP mice Develop Two GBM Variants

Overall, AscNP and AscNPP tumors displayed the classic histopathologic hallmarks of diffuse, infiltrating gliomas, primarily localized to the dorsal brain (telencephalon: cerebral cortex, hippocampus and caudate putamen; Figure 3A), and similar to the majority of gliomas derived from the neural stem cell-specific *Nestin-creER^{T2}* mutant mice (Alcantara Llaguno et al., 2009). Detailed scrutiny, however, revealed a subset of tumors that generally located to the ventral brain (diencephalon: thalamus and hypothalamus, and brainstem: midbrain, pons and medulla; Figure 3A) and tended to exhibit better-defined tumor borders (Figures 3B–3C). Compared to the more prevalent gliomas identified in these and previous studies (Alcantara Llaguno et al., 2009; Kwon et al., 2008; Zhu et al., 2005), the variant GBM subset uniformly showed reduced immunoreactivity for Gfap and Nestin coupled with enhanced Olig2 and Pdgfrα expression (Figures 3D–3E). Immunoreactivity to other lineage markers was similar for both tumor types (Figure S3A). When dissociated and grown in serum-free, growth factor-supplemented media, both GBM types displayed similar cell viability (Figure S3B). Hereafter, we refer to the predominant, Gfap^{high} tumors as Type 1 gliomas and the less frequent, Gfap^{low} variant tumors as Type 2 gliomas (Figure 3F).

Type 1 tumors are predominant in AscNPP mice while AscNP mice develop both tumor types equally (Figure 3G). One possible explanation may be that the presence of the Pten mutation in AscNPP elicits faster development of the more infiltrative and aggressive Type 1 tumors, thus, masking the development of Type 2 variant GBMs. Quantification of marker^{+} cells in tumor brain sections show increased proliferation (Ki67^{+}) and decreased apoptosis (cleaved caspase 3^{+}) in Type 1 compared to Type 2 tumors (Figures 3H–3I). These features are consistent with two GBM subtypes that exhibit morphologic and phenotypic differences.

Type 1 and 2 Gliomas Exhibit Characteristic Behavior In Vivo

We tested whether Type 1 and Type 2 glioma differences reflect intrinsic tumor cell properties or, alternatively, are influenced by microenvironment (anatomic location). We transplanted equal numbers of early passage AscNP Type 1 and Type 2 tumor cells from two independent lines into the dorsal striatum (a common Type 1 site) of immunodeficient mice (Figure 4A). We found that Type 1 tumors confer significantly shorter median survival compared to Type 2 tumors, reflective of their more aggressive nature (37 vs. 126 days post-transplantation; Figure 4B) and developed into correspondingly infiltrative, Gfap^{high}-expressing gliomas (Figures 4C–4D). On the other hand, the transplanted Type 2 cells adhered to their original properties, including relatively lower Gfap and Nestin, and higher Olig2 and Pdgfrα staining (Figures 4C–4D). Transplanted Type 1 tumor cells were also found extensively intercalated between Mbp^{+} myelin fibers, consistent with its infiltrative nature (Figures 4E–4F). Thus, Type 1 and Type 2 tumors behave cell autonomously, conserving their unique histological characteristics and intrinsically distinct growth behavior irrespective of microenvironment.

Molecular Differences in Adult CNS Progenitor-Driven Tumors

We next examined the gene expression profiles of AscNP primary gliomas and control tissue from dorsal (cortex and striatum) or ventral (hypothalamus and hindbrain) brain

regions of age-matched controls by microarray. Unsupervised hierarchical clustering analysis demonstrated clear delineation between tumor and control samples (Figure 5A). Dimension reduction analysis using the Locally Linear Embedding method projected the 2700 differentially expressed genes between tumors and controls (Figure 5A; Table S1) into 3-dimensional space and showed clustering of the Type 1 tumors separate from Type 2 tumors, as well as the dorsal and ventral control groups (Figure 5B). Direct comparison between the clustered Type 1 and Type 2 tumors showed clear separation, with differentially expressed genes involved in transcriptional regulation and neuronal development (Figures 5C–5D; Tables S2–S3).

We next compared the transcriptional profiles of AscNP tumors with different CNS cell populations using murine brain cell type-specific profiles defined by the Barres group (Cahoy et al., 2008). Unsupervised hierarchical clustering was applied to the gene expression profiles of AscNP Type 1 and Type 2 gliomas and control samples, as well as OPCs, differentiated oligodendrocytes, myelinating oligodendrocytes (Myelin OLs), astrocytes, and neurons. Clustering analysis best aligned Type 2 tumors with OPCs while Type 1 gliomas had relatively greater relatedness to astrocytes (Figure 5E). Taken together, these data show that Type 1 and 2 gliomas are molecularly distinct and give strength to the hypothesis that they arise from different cells of origin reflecting the two different progenitor lineages targeted by the *Ascl1-creER*^{TM} transgene.

Type 2 Gliomas are Adult OPC-Derived

To directly test the hypothesis that Type 2 tumors are derived from adult OPCs, we employed an OPC-specific *NG2-creER*^{TM} transgene (Zhu et al., 2011). Immunohistochemical analysis verified OPC specificity, including co-expression of the TdTomato reporter with the OPC marker Pdgfrα and mature oligodendrocyte marker APC, but not with NeuN, microglia marker Iba1, or Gfap (Figure 6A).

NG2-creER^{TM} with tumor suppressor conditional background (*NG2-creER*^{TM}*;Nf1*$^{flox/flox}$*;Trp53*$^{flox/flox}$*;Pten*$^{flox/+}$ or *NG2-creER*^{TM}*;Nf1*$^{flox/+}$*;Trp53*$^{flox/flox}$*;Pten*$^{flox/+}$; NG2NPP), and tamoxifen-induced at 4–8 weeks of age, had a median survival of 21.1 weeks (Fig. 6B), and developed WHO Grade III or IV gliomas (Figures 6C–6E). NG2NPP tumors showed histologic and molecular similarity to the Type 2 AscNP and AscNPP tumors (Figures 6D–6H), including the presence of pseudopalisading necrosis (Figure 6Ea), with low Gfap and Nestin, but high Pdgfrα and Olig2 immunoreactivity (Figures 6F, S4A). As observed for the Type 2 AscNP and AscNPP tumors, more NG2NPP tumors had better defined tumor borders compared to the more diffuse Type 1 tumors (Figures 6Ec–6Ed, 6G), and were preferentially found in ventral rather than dorsal brain (Figures 6D, 6H).

We next examined NG2NPP glioma gene expression profiles (Figures S4B–S4C). Similar to AscNP Type 2 tumors, clustering analysis of NG2NPP tumors with CNS cell type-specific gene profiles showed best alignment to OPCs (Figure 6I). Gene Set Enrichment Analysis (GSEA; Subramanian et al., 2005) comparing AscNP Type 1 and Type 2 tumors with NG2NPP tumors also showed higher normalized enrichment scores (NES), and hence, greater alignment with Type 2 gene sets compared to those of Type 1 (Table S4–S5). Thus,

Ascl1-creER^{TM} model Type 2 and *NG2-creER^{TM}* model tumors show greater relatedness, consistent with both tumors sharing OPCs as a common cell of origin.

GSEA was next used to examine the relatedness of Type 1 and 2 gliomas to molecular signatures of human glioblastoma (Verhaak et al., 2010). Differentially expressed genes from comparison of Ascl1 Type 1 vs. Type 2 tumors were derived and analyzed for enrichment of the TCGA human molecular subtype gene sets (Mesenchymal, Classical, Proneural and Neural) by GSEA. The data indicate that Type 1 tumors show higher enrichment scores than Type 2 for the Mesenchymal subtype gene sets (Table 1). These analyses are consistent with the notion that adult CNS progenitor-driven tumors exhibit similar genetic signatures as human high-grade gliomas and that these glioma variants represent molecularly distinct tumors.

Molecular Separation of Murine Gliomas Based on Cell of Origin

The *Ascl1-creER^{TM}* transgene drives tumor suppressor recombination in adult SVZ/SGZ neural progenitors and in adult OPCs, giving rise to both Type 1 and Type 2 gliomas, while the *NG2-creER^{TM}* transgene is confined to adult OPCs and only forms Type 2 gliomas. We turned to a third tamoxifen inducible transgene, *Nestin-creER^{T2}*, that recombines SVZ/SGZ neural stem and progenitor cell populations, and shows properties similar to Type 1 tumors (Alcantara Llaguno et al., 2009; Chen et al., 2009). Gene expression analysis of *Nestin-creER^{T2}* GBM (*Nestin-creER^{T2};Nf1$^{flox/+}$;Trp53$^{flox/flox}$;Pten$^{flox/+}$*; NesNPP) compared to Type 2-specific NG2NPP (*NG2-creER^{TM};Nf1*$^{flox/+}$;*Trp53*$^{flox/flox}$;*Pten*$^{flox/+}$) tumors revealed clear separation when plotted by LLE dimension reduction analysis (Figure 7A).

We then examined the transcriptional profiles of the three mouse models AscNP, NesNPP and NG2NPP. We first determined the similarity of the three tumor suppressor mouse models with those of human GBM, other human tumors of the CNS and other organ systems by GSEA (Sweet-Cordero et al., 2005). As shown in Table S6, the AscNP, NesNPP and NG2NPP mouse models exhibit the highest enrichment scores for human GBM, and not oligodendroglioma or other CNS or non-CNS tumors, indicating that the mouse models show the highest molecular similarity to human GBM.

We next analyzed published data comparing gene expression signatures of SVZ-derived stem cells vs. OPCs (Beckervordersandforth et al., 2010), and found 1249 differentially expressed genes from this data set (Table S7). Unsupervised hierarchical clustering analysis showed that NesNPP and Type 1 AscNP gliomas cluster together and separately from Type 2 gliomas derived from NG2NPP and AscNP models (Figure 7B). The heat map showing the top 310 differentially expressed genes with the highest median absolute deviation (MAD > 0.7; Table S8) not only demonstrate separation of Type 1 from Type 2 GBMs but also show unique expression patterns for all tumor subgroups as well as lineage-specific signatures for GBMs initiated from adult CNS stem cells, adult CNS Progenitors and adult OPCs.

Taken together, these microarray profiling data corroborate the model that at least two separable pools of glioma-initiating progenitors are susceptible to transformation by loss of identical human glioma-relevant tumor suppressors *Nf1*, *Trp53* and *Pten*, in the adult mouse

brain (Figure 7C). In addition to differing biological characteristics, the resultant GBMs conserve distinguishing molecular features reflecting their cells of origin. The development of two different glioblastoma subtypes derived from two different progenitor populations with the same initiating mutations show that, in addition to signature mutations and pathways, the cell of origin for tumor initiation can be an important determinant of GBM phenotype. Such findings in human GBM would have important implications for tumor molecular classification and treatment measures.

Discussion

Extensive molecular profiling of GBM has yielded an ever-refined genomic landscape (Dunn et al., 2012). These studies have led to a variety of criteria that stratify GBM into molecular subtypes (Phillips et al., 2006; Verhaak et al., 2010). However, functional experimental evidence that validates the existence of biologically different tumor subclasses lags behind.

The aim of the present study was to examine the tumorigenic potential of adult CNS committed progenitors and transit amplifying cells to form GBM. The results demonstrate that, indeed, adult CNS progenitor cells harboring the same glioma relevant mutations as applied to stem cells, can give rise to GBM efficiently. An unexpected result identified two pathologically similar but molecularly distinct GBM tumor types that arise from different cells of origin that normally specify separate adult lineages.

Thus, despite limited self-renewal and restricted differentiation potential, tumor suppressor deletion can initiate the tumorigenic cascade in two types of adult CNS progenitors. Similar to committed hematopoietic cells, the data indicate that adult neural and oligodendrocyte progenitors are also able to overcome programmed limitations necessary to engender glioma. In leukemias, oncogenes such as MLL have been shown to confer properties of enhanced self-renewal (Huntly et al., 2004), which allow transformed hematopoietic progenitors to self-renew indefinitely and acquire additional mutations. We observe early proliferation and differentiation defects in AscNP mutants, suggesting that tumor suppressor loss likewise leads to changes in intrinsic programming in transformed CNS progenitor cells.

It is also important to note that GBM is an adult disease with a median age of 64 years at time of diagnosis (Stupp et al., 2005; Wen and Kesari, 2008). In light of the known phenotypic differences between embryonic and adult cells (Kriegstein and Alvarez-Buylla, 2009), it is unlikely that spontaneous GBMs arise in embryonic cells, underscoring the importance of adult-induced glioma mouse models. Unlike studies that target cultured embryonic cells into mice that develop tumors almost immediately (Ghazi et al., 2012), we purposely used a variety of inducible transgenic mice that allow temporal control of gene ablation in adult brains.

The *Ascl1-creER*^{TM} transgene promotes LoxP recombination and GBM tumorigenesis in both adult neural and oligodendrocyte progenitors. However, two separable types of tumors emerge in AscNP and AscNPP mutants, with Type 1 GBMs resembling the majority of

gliomas found in the *Nestin-creER^{T2}* (Alcantara Llaguno et al., 2009) and *hGFAP-Cre* lines (Chen et al., 2012a; Kwon et al., 2008; Zhu et al., 2005), and a second subset of GBMs, designated as Type 2. The dual specificity of the *Ascl1-creER^{TM}* transgene to both types of progenitors raised the possibility that Type 2 GBMs arose from adult OPCs. We confirmed this hypothesis using the NG2NPP models.

The presence of Type 1-like tumors in the neural stem cell-specific NesNPP models, which molecularly clustered with Type 1 AscNP tumors, indicate that the *Nestin-creER^{T2}* model fate into the same cells as *Ascl1-creER^{TM}* adult neural progenitor cells. This suggests that the progenitor stage might be a common endpoint for transformed CNS cells, similar to findings in leukemia models (Cozzio et al., 2003). Retrospective analysis of the *hGFAP-Cre*-driven glioma models revealed that these mice also develop Type 2 gliomas, which became most apparent upon growth arrest of Type 1 tumors through HSV-thymidine kinase transgene-targeted killing of cancer stem cells (Chen et al., 2012a).

OPCs have also been implicated as cells of origin for another less frequent CNS malignancy, oligodendroglioma. Extensive analyses show that Type 2 GBMs are histologically, genetically, and molecularly most similar to GBM and are entirely different from oligodendroglioma, which do not associate with mutations in *NF1* or *TP53* (Ohgaki and Kleihues, 2005).

Our study identifies adult OPCs as a source for only one type of high-grade glioma, the Type 2 GBM. Zong and colleagues have induced gliomas by recombination of the *Nf1* and *Trp53* tumor suppressors in oligodendrocytic progenitors and found tumors that appear to be found in the ventral brain (Galvao et al., 2014; Liu et al., 2011). Taking the present results into consideration, it is likely that Zong and colleagues are modeling the Type 2 gliomas described here.

Dramatic advances in genomic technology has permitted molecular stratification of glioblastomas on the basis of gene transcription, copy number, chromosomal integrity, mutation spectrum, and related data (Li et al., 2012; Phillips et al., 2006; Verhaak et al., 2010). These compelling classifications have provided momentum to the notion that driver mutations and their molecular pathways define GBM subtypes. However, the clinical implications of these genome-based classifications remain less clear.

Our data point to a contrasting scenario in which identical GBM relevant driver mutations and pathways can promote biologically different tumor types based on the tumor cell of origin. Type 1 and 2 GBMs arise in different adult progenitor lineages and develop unique cell autonomous phenotypes, gene expression profiles, and natural history. Our mouse models suggest that GBM development and prognosis may reflect not only the sum of pathological features and the molecular driver genes, but equally or more so, the cell of origin in which the mutations arose. These observations are congruent with those of EWS-ATF1-induced clear cell sarcoma mouse models reported by the Capecchi group (Straessler et al., 2013). Thus, use of physiologically relevant glioma mouse models to directly target different brain cell populations using diverse mutations frequently found in GBM, may serve as complementary tools towards a more refined classification of tumor subtypes that takes

the cell of origin and functional analysis into consideration together with human clinical and genomic data.

Experimental Procedures

Additional details are available in Supplemental Experimental Procedures.

Mouse Experiments

All mouse experiments were approved and performed according to the guidelines of the Institutional Animal Care and Use Committee of the University of Texas Southwestern Medical Center at Dallas. Mice with the *Ascl1-creER^{TM}* (Kim et al., 2007), *NG2-creER^{TM}* (Zhu et al., 2011), or *Nestin-creER^{T2}* (Alcantara Llaguno et al., 2009; Chen et al., 2009) transgenes were crossed with conditional or null *Nf1*, *Trp53* and/or *Pten* alleles and the *R26-stop-lacZ*, *R26-stop-YFP* or *R26-stop-TdTomato* reporters. Tumor suppressor floxed mice containing the cre transgenes were administered with tamoxifen (Sigma) or vehicle by oral gavage at adult ages (4–8 weeks of age) and aged until symptomatic or at indicated time points.

Histology and Tumor Analysis

Brain sections were independently examined by S.A.L., Z.W., J.C., D.K.B., J.M.R. and K.J.H., the latter three being certified neuropathologists, and tumor diagnosis was determined based on the World Health Organization criteria (Louis et al., 2007). PCR genotyping and Western blot analysis using tumor and non-tumor tissues and/or cells, were performed as previously described (Kwon et al., 2008). Paraffin or vibratome brain sections were analyzed by H&E and X-gal staining, as well as fluorescence and horseradish peroxidase-based immunostaining, as previously described (Alcantara Llaguno et al., 2009).

Tissue Culture and Transplantations

Primary tumor tissues were freshly dissected from symptomatic mutant mice while SVZ from age-matched mice were used as controls. Harvested tissues were minced into single cell suspension and grown as neurospheres. Self-renewal, differentiation and ATP assays were performed as previously described (Alcantara Llaguno et al., 2009).

For transplantation experiments, 4-week-old female *nu/nu* mice were anesthetized and directly injected with 2×10^5 tumor cells into the dorsal striatum (coordinates: 0 AP, 1.4 ML, 2.3 DV with respect to the bregma). Mice were aged until symptomatic.

Gene Expression Profile Analysis

Primary tumor tissue and respective control brains were harvested from symptomatic AscNP, NG2NPP and NesNPP mutants and control mice. Total RNA extracted from samples was submitted to the UT Southwestern Microarray Core for analysis using Illumina WG-6 V2 BeadChips. Statistical analysis of microarray data is described in greater detail in Supplemental Experimental Procedures. Gene expression data was deposited in Gene Expression Omnibus with GEO accession numbers GSE57036 and GSE57038.

Supplementary Material

Refer to Web version on PubMed Central for supplementary material.

Acknowledgments

The authors thank members of the Parada lab for helpful suggestions and discussion. *NG2-creER*^{TM} mice were acquired from Dr. Akiko Nishiyama. This work was supported in part by Children's Tumor Foundation Young Investigator Award and NIH T32 Postdoctoral Trainee support (2T32CA124334-06; PI: Jerry Shay) to S.R.A.L. L.F.P. is an American Cancer Society Research Professor and recipient of NIH R01 grant CA131313-01A1 and Cancer Prevention and Research Institute of Texas Grant RP100782.

References

Alcantara Llaguno S, Chen J, Kwon CH, Jackson EL, Li Y, Burns DK, Alvarez-Buylla A, Parada LF. Malignant astrocytomas originate from neural stem/progenitor cells in a somatic tumor suppressor mouse model. Cancer Cell. 2009; 15:45–56. [PubMed: 19111880]

Alvarez-Buylla A, Lim DA. For the long run: maintaining germinal niches in the adult brain. Neuron. 2004; 41:683–686. [PubMed: 15003168]

Beckervordersandforth R, Tripathi P, Ninkovic J, Bayam E, Lepier A, Stempfhuber B, Kirchhoff F, Hirrlinger J, Haslinger A, Lie DC, et al. In vivo fate mapping and expression analysis reveals molecular hallmarks of prospectively isolated adult neural stem cells. Cell Stem Cell. 2010; 7:744–758. [PubMed: 21112568]

Cahoy JD, Emery B, Kaushal A, Foo LC, Zamanian JL, Christopherson KS, Xing Y, Lubischer JL, Krieg PA, Krupenko SA, et al. A transcriptome database for astrocytes, neurons, and oligodendrocytes: a new resource for understanding brain development and function. J Neurosci. 2008; 28:264–278. [PubMed: 18171944]

Chen J, Kwon CH, Lin L, Li Y, Parada LF. Inducible site-specific recombination in neural stem/progenitor cells. Genesis. 2009; 47:122–131. [PubMed: 19117051]

Chen J, Li Y, Yu TS, McKay RM, Burns DK, Kernie SG, Parada LF. A restricted cell population propagates glioblastoma growth after chemotherapy. Nature. 2012a; 488:522–526. [PubMed: 22854781]

Chen J, McKay RM, Parada LF. Malignant glioma: lessons from genomics, mouse models, and stem cells. Cell. 2012b; 149:36–47. [PubMed: 22464322]

Cozzio A, Passegue E, Ayton PM, Karsunky H, Cleary ML, Weissman IL. Similar MLL-associated leukemias arising from self-renewing stem cells and short-lived myeloid progenitors. Genes Dev. 2003; 17:3029–3035. [PubMed: 14701873]

Doetsch F, Caille I, Lim DA, Garcia-Verdugo JM, Alvarez-Buylla A. Subventricular zone astrocytes are neural stem cells in the adult mammalian brain. Cell. 1999; 97:703–716. [PubMed: 10380923]

Dunn GP, Rinne ML, Wykosky J, Genovese G, Quayle SN, Dunn IF, Agarwalla PK, Chheda MG, Campos B, Wang A, et al. Emerging insights into the molecular and cellular basis of glioblastoma. Genes Dev. 2012; 26:756–784. [PubMed: 22508724]

Friedmann-Morvinski D, Bushong EA, Ke E, Soda Y, Marumoto T, Singer O, Ellisman MH, Verma IM. Dedifferentiation of neurons and astrocytes by oncogenes can induce gliomas in mice. Science. 2012; 338:1080–1084. [PubMed: 23087000]

Galvao RP, Kasina A, McNeill RS, Harbin JE, Foreman O, Verhaak RG, Nishiyama A, Miller CR, Zong H. Transformation of quiescent adult oligodendrocyte precursor cells into malignant glioma through a multistep reactivation process. Proc Natl Acad Sci U S A. 2014; 111:E4214–4223. [PubMed: 25246577]

Ghazi SO, Stark M, Zhao Z, Mobley BC, Munden A, Hover L, Abel TW. Cell of origin determines tumor phenotype in an oncogenic Ras/p53 knockout transgenic model of high-grade glioma. J Neuropathol Exp Neurol. 2012; 71:729–740. [PubMed: 22805776]

Huntly BJ, Shigematsu H, Deguchi K, Lee BH, Mizuno S, Duclos N, Rowan R, Amaral S, Curley D, Williams IR, et al. MOZ-TIF2, but not BCR-ABL, confers properties of leukemic stem cells to

committed murine hematopoietic progenitors. Cancer Cell. 2004; 6:587–596. [PubMed: 15607963]

Jacques TS, Swales A, Brzozowski MJ, Henriquez NV, Linehan JM, Mirzadeh Z, COM, Naumann H, Alvarez-Buylla A, Brandner S. Combinations of genetic mutations in the adult neural stem cell compartment determine brain tumour phenotypes. Embo J. 2010; 29:222–235. [PubMed: 19927122]

Kim EJ, Battiste J, Nakagawa Y, Johnson JE. Ascl1 (Mash1) lineage cells contribute to discrete cell populations in CNS architecture. Mol Cell Neurosci. 2008; 38:595–606. [PubMed: 18585058]

Kim EJ, Leung CT, Reed RR, Johnson JE. In vivo analysis of Ascl1 defined progenitors reveals distinct developmental dynamics during adult neurogenesis and gliogenesis. J Neurosci. 2007; 27:12764–12774. [PubMed: 18032648]

Kriegstein A, Alvarez-Buylla A. The glial nature of embryonic and adult neural stem cells. Annu Rev Neurosci. 2009; 32:149–184. [PubMed: 19555289]

Krivtsov AV, Twomey D, Feng Z, Stubbs MC, Wang Y, Faber J, Levine JE, Wang J, Hahn WC, Gilliland DG, et al. Transformation from committed progenitor to leukaemia stem cell initiated by MLL-AF9. Nature. 2006; 442:818–822. [PubMed: 16862118]

Kwon CH, Zhao D, Chen J, Alcantara S, Li Y, Burns DK, Mason RP, Lee EY, Wu H, Parada LF. Pten haploinsufficiency accelerates formation of high-grade astrocytomas. Cancer Res. 2008; 68:3286–3294. [PubMed: 18451155]

Li B, Senbabaoglu Y, Peng W, Yang ML, Xu J, Li JZ. Genomic estimates of aneuploid content in glioblastoma multiforme and improved classification. Clin Cancer Res. 2012; 18:5595–5605. [PubMed: 22912392]

Lillien L. Neural progenitors and stem cells: mechanisms of progenitor heterogeneity. Curr Opin Neurobiol. 1998; 8:37–44. [PubMed: 9568390]

Liu C, Sage JC, Miller MR, Verhaak RG, Hippenmeyer S, Vogel H, Foreman O, Bronson RT, Nishiyama A, Luo L, Zong H. Mosaic analysis with double markers reveals tumor cell of origin in glioma. Cell. 2011; 146:209–221. [PubMed: 21737130]

Louis DN, Ohgaki H, Wiestler OD, Cavenee WK, Burger PC, Jouvet A, Scheithauer BW, Kleihues P. The 2007 WHO classification of tumours of the central nervous system. Acta Neuropathol. 2007; 114:97–109. [PubMed: 17618441]

Mich JK, Signer RA, Nakada D, Pineda A, Burgess RJ, Vue TY, Johnson JE, Morrison SJ. Prospective identification of functionally distinct stem cells and neurosphere-initiating cells in adult mouse forebrain. Elife. 2014; 3:e02669. [PubMed: 24843006]

Nishiyama A, Komitova M, Suzuki R, Zhu X. Polydendrocytes (NG2 cells): multifunctional cells with lineage plasticity. Nat Rev Neurosci. 2009; 10:9–22. [PubMed: 19096367]

Ohgaki H, Kleihues P. Population-based studies on incidence, survival rates, and genetic alterations in astrocytic and oligodendroglial gliomas. J Neuropathol Exp Neurol. 2005; 64:479–489. [PubMed: 15977639]

Phillips HS, Kharbanda S, Chen R, Forrest WF, Soriano RH, Wu TD, Misra A, Nigro JM, Colman H, Soroceanu L, et al. Molecular subclasses of high-grade glioma predict prognosis, delineate a pattern of disease progression, and resemble stages in neurogenesis. Cancer Cell. 2006; 9:157–173. [PubMed: 16530701]

Reya T, Morrison SJ, Clarke MF, Weissman IL. Stem cells, cancer, and cancer stem cells. Nature. 2001; 414:105–111. [PubMed: 11689955]

Sanai N, Alvarez-Buylla A, Berger MS. Neural stem cells and the origin of gliomas. N Engl J Med. 2005; 353:811–822. [PubMed: 16120861]

Sell S. On the stem cell origin of cancer. Am J Pathol. 2010; 176:2584–2494. [PubMed: 20431026]

Straessler KM, Jones KB, Hu H, Jin H, van de Rijn M, Capecchi MR. Modeling clear cell sarcomagenesis in the mouse: cell of origin differentiation state impacts tumor characteristics. Cancer Cell. 2013; 23:215–227. [PubMed: 23410975]

Stupp R, Mason WP, van den Bent MJ, Weller M, Fisher B, Taphoorn MJ, Belanger K, Brandes AA, Marosi C, Bogdahn U, et al. Radiotherapy plus concomitant and adjuvant temozolomide for glioblastoma. N Engl J Med. 2005; 352:987–996. [PubMed: 15758009]

Subramanian A, Tamayo P, Mootha VK, Mukherjee S, Ebert BL, Gillette MA, Paulovich A, Pomeroy SL, Golub TR, Lander ES, Mesirov JP. Gene set enrichment analysis: a knowledge-based approach for interpreting genome-wide expression profiles. Proc Natl Acad Sci U S A. 2005; 102:15545–15550. [PubMed: 16199517]

Sweet-Cordero A, Mukherjee S, Subramanian A, You H, Roix JJ, Ladd-Acosta C, Mesirov J, Golub TR, Jacks T. An oncogenic KRAS2 expression signature identified by cross-species gene-expression analysis. Nat Genet. 2005; 37:48–55. [PubMed: 15608639]

TCGA. Comprehensive genomic characterization defines human glioblastoma genes and core pathways. Nature. 2008; 455:1061–1068. [PubMed: 18772890]

Verhaak RG, Hoadley KA, Purdom E, Wang V, Qi Y, Wilkerson MD, Miller CR, Ding L, Golub T, Mesirov JP, et al. Integrated genomic analysis identifies clinically relevant subtypes of glioblastoma characterized by abnormalities in PDGFRA, IDH1, EGFR, and NF1. Cancer Cell. 2010; 17:98–110. [PubMed: 20129251]

Visvader JE. Cells of origin in cancer. Nature. 2011; 469:314–322. [PubMed: 21248838]

Wen PY, Kesari S. Malignant gliomas in adults. N Engl J Med. 2008; 359:492–507. [PubMed: 18669428]

Zhao C, Deng W, Gage FH. Mechanisms and functional implications of adult neurogenesis. Cell. 2008; 132:645–660. [PubMed: 18295581]

Zhu X, Hill RA, Dietrich D, Komitova M, Suzuki R, Nishiyama A. Age-dependent fate and lineage restriction of single NG2 cells. Development. 2011; 138:745–753. [PubMed: 21266410]

Zhu Y, Guignard F, Zhao D, Liu L, Burns DK, Mason RP, Messing A, Parada LF. Early inactivation of p53 tumor suppressor gene cooperating with NF1 loss induces malignant astrocytoma. Cancer Cell. 2005; 8:119–130. [PubMed: 16098465]

Significance

The cell of origin, including the role of adult lineage restricted progenitors in glioblastoma, is an area of ongoing controversy. Emerging human genomic data have been used to stratify GBM into subgroups. Identification of the CNS cell lineages that contribute to GBM using cell type-specific mouse models provides unique insight into mechanisms of tumor initiation and progression. Our findings showing different adult CNS progenitors as GBM-initiating cells and the cell of origin as a major driver of tumor subtype has important implications for functional subclassification of GBM and identification of subtype relevant target pathways.

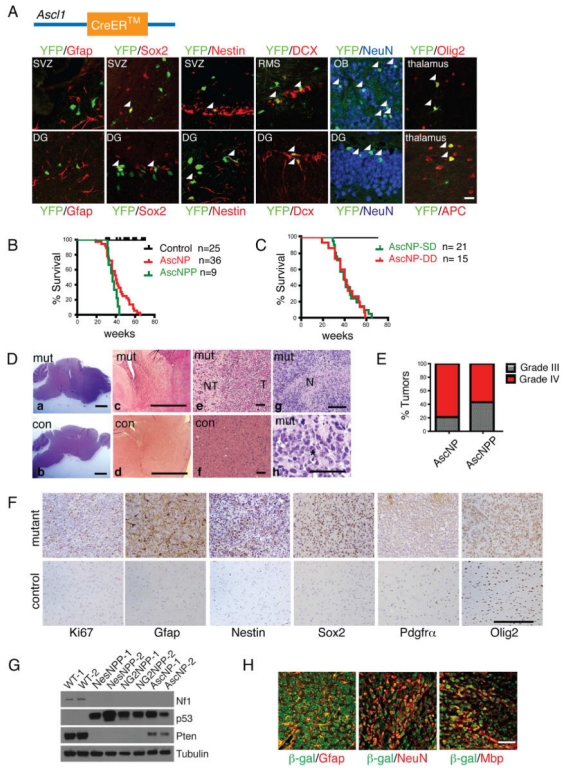

Figure 1. Tumor suppressor inactivation in adult lineage restricted CNS progenitors but not stem cells initiates GBM

(**A)** Schematic of *Ascl1-creER*^{TM} transgene (top). Immunohistochemical staining of *Ascl1-creER*^{TM}*;R26-stop-YFP* reporter adult mouse brain sections for YFP together with the neural stem cell–specific marker Gfap, neural stem/progenitor markers Sox2 and Nestin, immature neuronal marker doublecortin (Dcx), mature neuronal marker NeuN, OPC marker Olig2, and mature oligodendrocyte marker APC. Arrowheads mark YFP/marker co-localization. Scale bar: 20 μm (**B)** Kaplan-Meier survival curves of AscNP and AscNPP mice induced with tamoxifen at 4 weeks of age. Median survival: AscNP, 40 weeks; AscNPP, 36.7 weeks; p=0.0782. (**C**) Kaplan-Meier survival curves of AscNP mice induced with a single dose (SD) or double dose (DD) of tamoxifen. Median survival: SD, 39 weeks; DD, 33.5 weeks p=0.8044. **(D)** Representative H&E brain sections of AscNP and AscNPP mutant (mut) brains compared to controls (con; a–f). High-grade gliomas with characteristic features: indistinct tumor borders, with tumor cells (T) diffusely infiltrating into adjacent normal (NT) regions (e), pseudopalisading necrosis (N; g) and presence of mitotic figures (asterisk; h) are shown. Scale bars: a–b=1 mm; c–h=100 μm**. (E)** Bar graph showing percentage of AscNP and AscNPP tumors classified as WHO grade III or IV gliomas (n=16 AscNP, n=9 AscNPP mice). **(F)** Expression of high-grade glioma markers such as Ki67, Gfap, Nestin and Olig2, as well as progenitor markers Sox2 and Pdgfrα in AscNP and AscNPP tumors. Scale bar: 200 μm. **(G)** Western blot analysis of Nf1, p53, and Pten in AscNP, NG2NPP, and NesNPP tumors. Tubulin is used as a loading control. **(H)** Expression of mature differentiation markers (Gfap for astrocytes, NeuN for neurons, and myelin basic

protein or Mbp for oligodendrocytes) in a subset of β-galactosidase positive (cre^+) tumor cells in AscNP tumors with *R26-stop-lacZ* reporter. Scale bar: 100 μm. See also Figure S1.

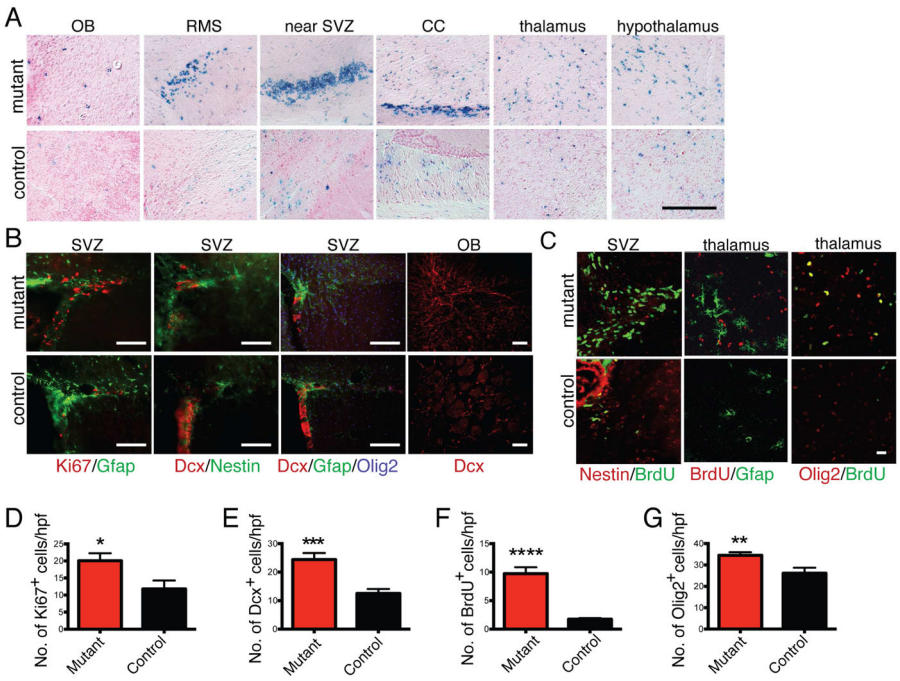

Figure 2. Increased proliferation and accelerated differentiation precede tumor formation

(A) AscNP *R26-stop-lacZ* and control reporter mice were administered tamoxifen at 4 weeks of age and analyzed 4 months later by X-gal staining. CC: corpus callosum. Scale bar: 200 μm. (**B**) Proliferation (based on Ki67 staining) and expression of various markers (Gfap, Nestin, Doublecortin, Olig2) in the SVZ and OB of AscNP and control brains. Scale bars: 200 μm. (**C**) Immunohistochemistry with BrdU and progenitor markers following short term BrdU pulses. Scale bar: 20 μm. (**D**) Quantification of $Ki67^+$ cells in SVZ (n=4 mutants, 4 controls; $p<0.05$). (**E**) Quantification of Dcx^+ cells in OB (n=4 mutants, 4 controls; $p=0.0001$). (**F**) Quantification of $BrdU^+$ cells in thalamus (n=3 mutants, 3 controls; $p<0.0001$). (**G**) Quantification of $Olig2^+$ cells in thalamus (n=3 mutants, 3 controls; $p<0.01$). All statistical analyses used Student's t test. All error bars denote mean ± SEM. See also Figure S2.

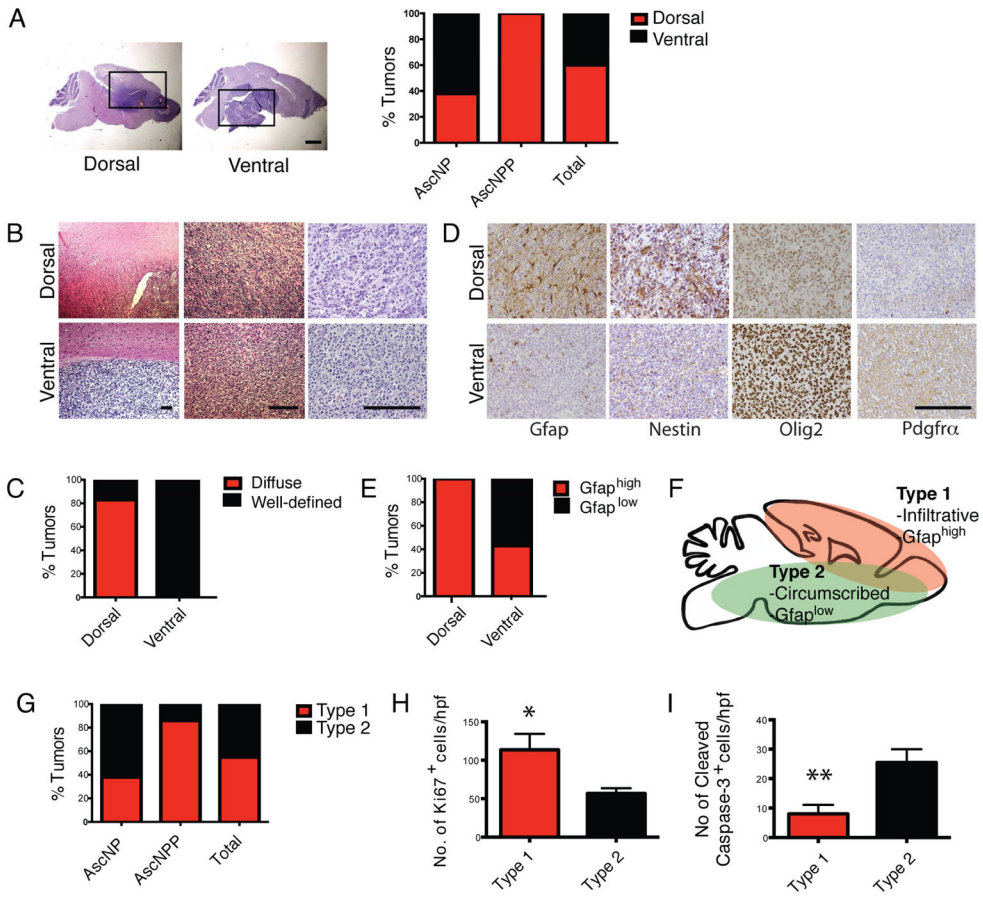

Figure 3. AscNP and AscNPP Mutants form Two Identifiable GBM Subtypes

(**A**) Left panels: Representative H&E staining images of AscNP and AscNPP brain sections showing a subgroup of gliomas in the dorsal brain and another subgroup found in ventral/basal region. Black boxes mark tumor regions. Scale bar: 1 mm. Right panel: Bar graph showing the percentage of gliomas in the dorsal and ventral brain regions that were identified in AscNP (n=13) and AscNPP (n=7) mutants. (**B**) H&E staining images of mutant brains showing tumor borders, at three different magnifications. Scale bars: 200 μM. (**C**) Bar graph showing the percentage of tumors that exhibit diffuse vs. well-defined tumor borders in dorsal (n=12) and ventral (n=8) tumors found in AscNP and AscNPP mice. (**D**) Immunohistochemistry of GBM markers in glioma subtypes found in AscNP and AscNPP mice. Scale bar: 200 μM. (**E)** Bar graph showing the percentage of dorsal (n=12) and ventral (n=8) tumors that shows high vs. low Gfap expression. (**F)** Schematic showing the general features of Type 1 vs. Type 2 gliomas. Type 1 gliomas are mostly diffuse tumors commonly found in the dorsal brain and exhibit high Gfap expression. Type 2 tumors are generally found in the ventral brain, show well-defined tumor borders, and exhibit low Gfap expression. (**G)** Bar graph showing the percentage of Type 1 and 2 tumors in AscNP (n=13) and AscNPP (n=7) mouse models. (**H)** Quantification of $Ki67^+$ cells per high power field (20x magnification; n=4 Type 1 tumors, n=4 Type 2 tumors; $p<0.05$). (**I**) Quantification of Cleaved $Caspase\text{-}3^+$ cells per high power field (20x magnification; n=3 Type 1 tumors, n=5

Type 2 tumors; $p<0.005$). All statistical analyses used Student's t test. All error bars denote mean ± SEM. See also Figure S3.

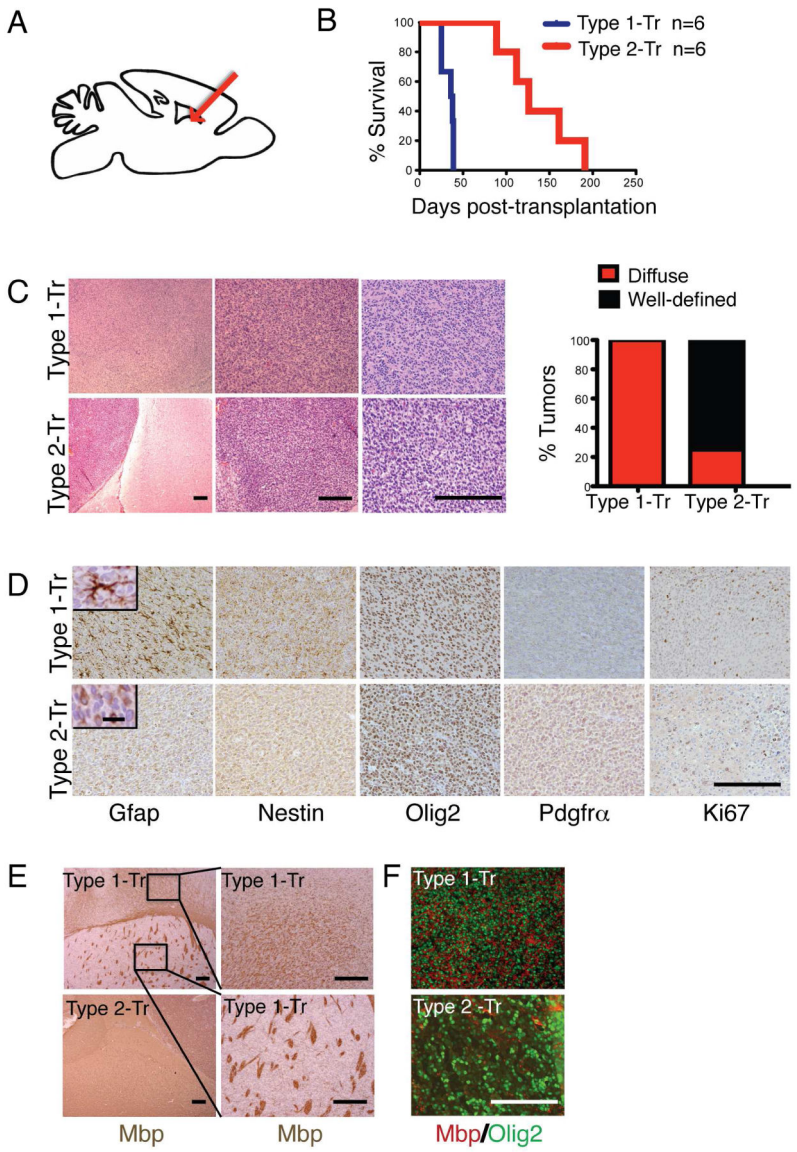

Figure 4. Differential Growth of Transplanted Type 1 and Type 2 GBM Cells

(A) Schematic of transplantation experiments. Type 1 and Type 2 tumors from symptomatic AscNP mice were cultured in serum-free media with growth factors and 2×10^5 tumor cells were subsequently transplanted into the dorsal striatum (arrow) of adult immunodeficient mice. (**B**) Kaplan-Meier survival curve of nude mice transplanted with Type 1 (n=6) compared with Type 2 tumor cells (n=6); $p<0.01$. Two independent lines for each tumor subtype were tested. Figure shows a representative survival curve for the independent lines used for each type. (**C**) H&E staining of tumors from Type 1 vs. Type 2 transplanted mice, and bar graph showing percentage of transplanted tumors with diffuse or well-defined tumor borders (n=6 tumors for each type analyzed). Scale bars: 200 μm. (**D**) Immunohistochemical staining using glioma markers. Scale bar: 200 μm. Insets show higher magnification images of Gfap staining (scale bar: 20 μm). **(E)** Mbp staining showing association with myelin fibers and fiber bundles in tumor regions of Type 1 vs. Type 2 transplanted mice. Right sub-

panels show higher magnification images of a Type 1 tumor in the cortex (top) and striatum (bottom). Scale bars: 200 μm. (**F**) Immunofluoresence staining for Olig2 (tumor cells) and Mbp within the tumor bulk of Type 1 and Type 2 transplanted gliomas. Scale bars: 200 μm.

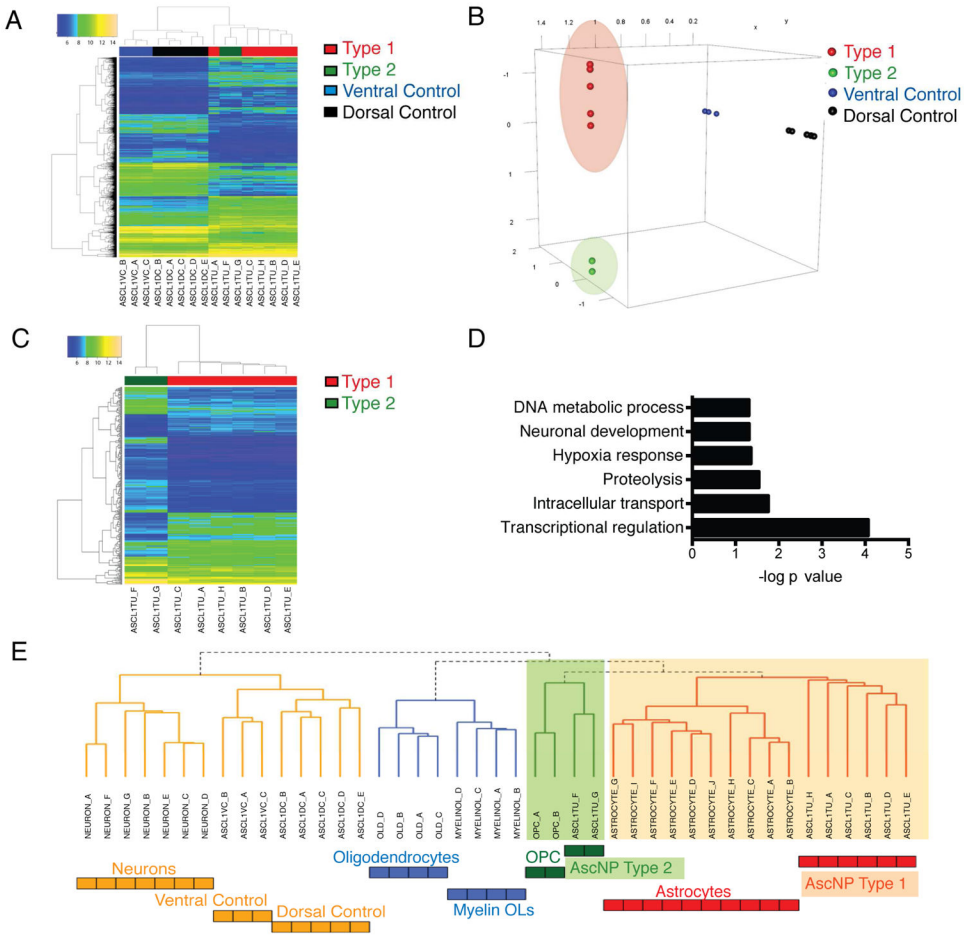

Figure 5. Distinguishable Molecular Signatures for Type 1 and Type 2 Gliomas

(**A**) Heat map of 2700 differentially expressed genes (DEGs) between AscNP tumors (n=8) and controls (n=8) and the result of unsupervised hierarchical clustering analysis. (**B**) Locally Linear Embedding (LLE) dimension reduction analysis depicting the DEGs projected in 3-dimensional space and showing separated groups of dorsal and ventral tissue controls as well as Type 1 and Type 2 gliomas (outlier removed). (**C**) Heat map of DEGs by direct comparison of AscNP Type 2 tumors with Type 1 tumors. (**D**) Gene Ontology Analysis of DEGs between Type 1 and 2 tumors. (**E**) Unsupervised hierarchical cluster analysis of gene expression profiles of Type 1 and 2 gliomas in comparison with different adult murine CNS cell states (derived from Cahoy et al., 2008). See also Tables S1–S3.

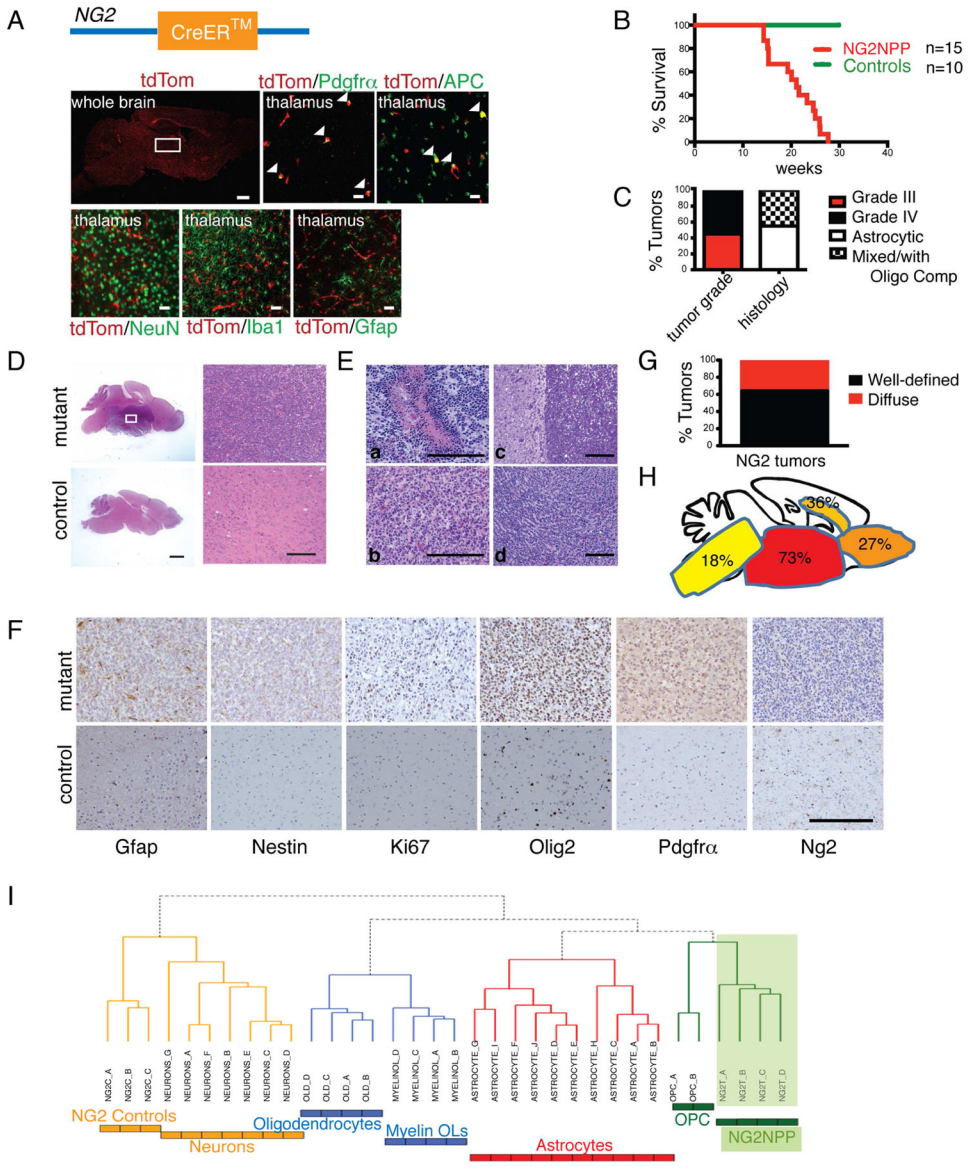

Figure 6. Adult Oligodendrocyte Progenitors are the Source of Type 2 GBM

(**A**) *NG2-creER*^{TM} transgene schematic (top). Immunohistochemical staining of *NG2-creER*^{TM}*;R26-stop-TdTomato* reporter together with OPC marker Pdgfrα, mature oligodendrocyte marker APC, neuronal marker NeuN, microglial marker Iba1 and astrocytic marker Gfap in OPC regions such as the thalamus (area denoted by white box in whole brain image). Arrowheads indicate co-localization of TdTomato with indicated marker. Scale bars: whole brain, 500 μm; all other sub-panels, 20 μm. (**B**) Kaplan-Meier survival curve of NG2NPP mice tamoxifen-induced at 4–8 weeks and aged until symptomatic (n=15 NG2NPP, 10 Controls). (**C**) Bar graph showing percentage of NG2NPP tumors classified as either WHO Grade III (n=5) or IV (n=6) gliomas or classified as malignant astrocytomas (n=6) or mixed differentiation gliomas (Anaplastic Oligoastrocytomas or Glioblastoma with Oligodendroglioma Component (GBMO); n=5). (**D**) Representative H&E staining of a histologically identifiable high-grade glioma in a symptomatic NG2NPP mutant mouse

compared to a control mouse brain. White box indicates the tumor region magnified in the right top sub-panel; right bottom sub-panel shows the corresponding region in control brain. Scale bars: left two sub-panels, 1 mm; right two sub-panels, 200 μm. (**E**) Representative H&E staining of Grade IV tumors in NG2NPP mutant mice showing pseudopalisading necrosis (a), oligodendrocytic differentiation (b), circumscribed tumor with a clear boundary (c), and tumor with less defined borders (d). Scale bars: 200 μm. (**F**) Immunohistochemistry indicating expression of different markers in NG2NPP tumors. Scale bar: 200 μm. (**G**) Bar graph showing percentage of NG2NPP gliomas that exhibit lesions with identifiable borders (n=7 well-defined vs. n=4 diffuse). (**H**) Frequency of tumor locations in NG2NPP tumors. (**I)** Clustering Analysis of NG2NPP tumors with adult murine CNS cell types showing relatedness to OPCs. See also Figure S4 and Tables S4–S5.

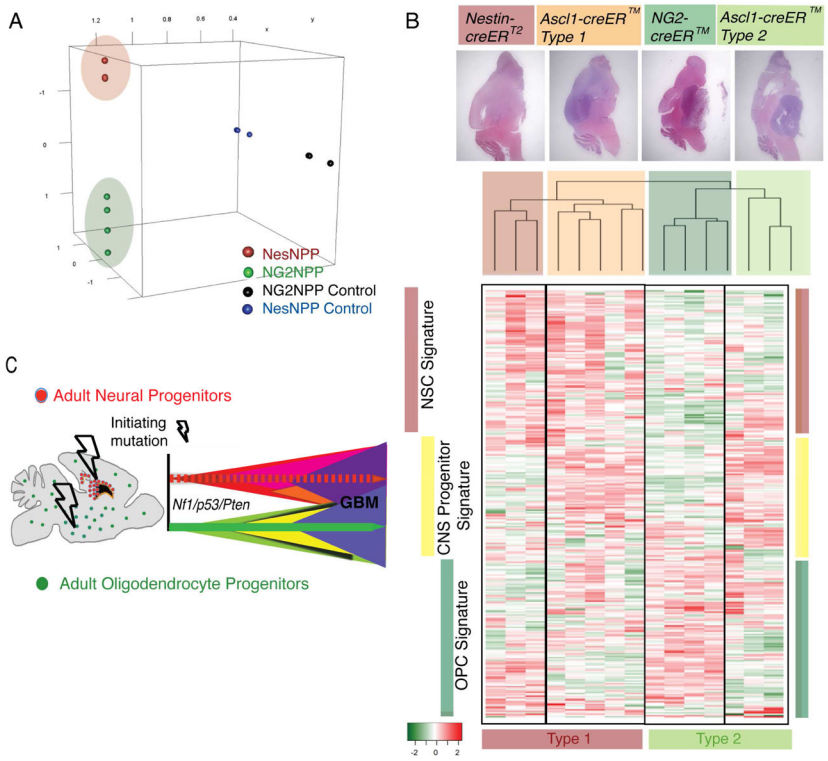

Figure 7. Molecular Separation of Mouse Gliomas based on Cell of Origin

(A) LLE dimension reduction analysis showing the expression of 18,000+ genes probed by microarray and projected in 3-dimensional space in NesNPP and NG2NPP mouse models and their controls. (B) Analysis of mouse model gene expression profiles based on cell of origin. Top panels show representative tumors derived from *Ascl1-creER^{TM}* (Type 1 and 2 tumors shown), *Nestin-creER^{T2}* and *NG2-creER^{TM}* models. Unsupervised hierarchical clustering analysis of AscNP, NesNPP and NG2NPP tumors using differentially expressed genes from published data comparing SVZ neural stem cells and OPCs (Beckervordersandforth et al., 2010). Heat map represents the gene expression profile of the top 310 differentially expressed genes with the highest median absolute deviation (MAD >0.7) showing the molecular separation of the mouse model tumors based on the tumor-initiating cell. Side bars indicate lineage-specific signatures that highlight distinct expression patterns by GBMs derived from NSCs (NesNPP), Progenitors (AscNP Type 1 and 2) and OPCs (NG2NPP). Bottom bars emphasize the common Type 1 (NesNPP and AscNP Type 1) and Type 2 (NG2NPP and AscNP Type 2) tumors. **(C)** Model of adult progenitor cell of origin of gliomas. Our studies are consistent with the presence of at least two distinct lineages of GBM-initiating progenitors in the adult mouse brain. GBMs show overlapping histologic similarity but retain molecular differences arising from different cellular origins. See also Tables S6–S8.

Table 1

Human Glioblastoma Subtype Gene Sets Enriched in Ascl1 Type 1 vs. Type 2 Tumors.

Human GBM Molecular Subtype Gene Sets (TCGA)	Ascl1 Type 1 vs. Type 2 Phenotype Data Set			
	ES	NES	NOM p value	FDR q value
Mesenchymal	0.55	1.80	0.000	0.000
Classical	0.36	1.16	0.154	0.310
Proneural	0.36	1.14	0.192	0.246
Neural	0.33	1.05	0.331	0.347

Abbreviations: ES=enrichment score; NES=normalized enrichment score; NOM p value=nominal p value; FDR q value=false discovery rate q value